# Causal relationship between the right auditory cortex and speech-evoked frequency-following response: Evidence from combined tDCS and EEG

Guangting Mai[1,*], Peter Howell[1,*]

[1]Department of Experimental Psychology, University College London, London, UK, WC1H 0AP

**Correspondence:** guangting.mai.15@ucl.ac.uk (G.M.); p.howell@ucl.ac.uk (P.H.)

**Abbreviated title:** Causal relation between auditory cortex and FFR

**Conflict of interest:** The authors declare no competing financial interests

**Author contributions:** G.M. designed research, performed research, and analysed the data; P.H. provided laboratory resources and supervised the study; G.M. drafted the manuscript; both authors contributed to writing, editing and approving the paper.

# Abstract

Speech-evoked frequency-following response (FFR) reflects the neural encoding of speech periodic information in the human auditory systems. FFR is of fundamental importance for pitch and speech perception and serves as clinical biomarkers for various auditory and language disorders. While it is suggested that the main neural source of FFR is in the auditory brainstem, recent studies have shown a cortical contribution to FFR predominantly in the right hemisphere. However, it is still unclear whether auditory cortex and FFR are causally related. The aim of this study was to establish this causal relationship using a combination of transcranial direct current stimulation (tDCS) and scalp-recorded electroencephalography (EEG). We applied tDCS over the left and right auditory cortices in right-handed normal-hearing participants and examined the after-effects of tDCS on FFR using EEG during monaural listening to a repeatedly-presented speech syllable. Our results showed that: (1) before tDCS was applied, participants had greater FFR magnitude when they listened to speech from the left than the right ear, illustrating right-lateralized hemispheric asymmetry for FFR; (2) anodal and cathodal tDCS applied over the right, but not left, auditory cortex significantly changed FFR magnitudes compared to the sham stimulation; specifically, such after-effects occurred only when participants listened to speech from the left ear, emphasizing the right auditory cortical contributions along the contralateral pathway. The current finding thus provides the first causal evidence that validates the relationship between the right auditory cortex and speech-evoked FFR and should significantly extend our understanding of speech encoding in the brain.

# Significance Statement

Speech-evoked frequency-following response (FFR) is a neural activity that reflects the brain's encoding of speech periodic features. The FFR has great fundamental and clinical importance for auditory processing. Whilst convention maintains that FFR derives mainly from the brainstem, it has been argued recently that there are additional contributions to FFR from the auditory cortex. Using a combination of tDCS, that altered neural excitability of auditory cortices, and EEG recording, the present study provided the first evidence to validate a causal relationship between the right auditory cortex and speech-evoked FFR. The finding supports the right-asymmetric auditory cortical contributions to processing of speech periodicity and

56  advances our understanding of how speech signals are encoded and analysed along the central

57  auditory pathways.

58

# Introduction

60      Speech-evoked frequency-following response (FFR) is a phase-locked neural activity

61  that reflects early processing of periodic features of input speech signals in the human brain

62  (Picton and Aiken, 2008; Coffey et al., 2019).

63      The FFR is closely related to fundamental auditory processes. For instance, it plays an

64  important role in pitch perception. FFR reflects the neural fidelity of linguistic pitch and is

65  stronger in tonal language than non-tonal language speakers (Krishnan et al., 2004, 2005,

66  2009). It has greater strength in musicians who have better pitch discrimination ability than

67  people without musical training (Musacchia et al., 2007; Wong et al., 2007; Strait et al., 2009;

68  Bidelman et al., 2011). Furthermore, FFR is important for speech-in-noise perception. Greater

69  FFR magnitudes are associated with better speech recognition ability in noisy environments

70  (Song et al., 2011; Parbery-Clark et al., 2011). FFR also reflects neural plasticity related to

71  fundamental cognitive and physiological processes such as auditory learning (Skoe et al.,

72  2014), changes in arousal (Mai et al., 2019) and attention (Lehmann and Schönwiesner, 2014;

73  Hartmann and Weisz, 2019).

74      Clinically, FFR is proposed as a biomarker for various auditory and language disorders.

75  FFR declines with age (Anderson et al., 2012; Presacco et al., 2016) and can predict word

76  recognition ability during speech-in-noise perception in older adults (Anderson et al., 2011;

77  Fujihira and Shiraishi, 2015; Mai et al., 2018). This indicates that degradations to FFR could

78  potentially explain the increased speech-in-noise difficulty experienced during aging. FFRs are

79  also associated with hearing deficits such as cochlear synaptopathy (Encina-Llamas et al.,

80  2019) and auditory processing disorders (Schochat et al., 2017). Furthermore, FFR is a

81  potential marker for detecting functional impairments in learning and cognitive disorders in

82  children, such as learning difficulties in literacy (Cunningham et al., 2001; Banai et al., 2007;

83  White-Schwoch et al., 2015), dyslexia (Hornickel et al., 2013) and autism (Russo et al., 2008).

84      It is argued that the fundamental and clinical importance of FFR is linked to the neural

85  fidelity of speech in the inferior colliculus at the brainstem, which has been proposed as the

86    main neural origin of FFR (Chandrasekaran and Kraus, 2010; Bidelman, 2015, 2018). Recent

87    studies, however, have shown an additional source of FFR in the right auditory cortex

88    associated with musical experience, pitch discrimination ability (Coffey et al., 2016), speech-

89    in-noise perception (Coffey et al., 2017a) and intermodal attention (Hartmann and Weisz,

90    2019). FFR strength is associated with right-lateralized hemodynamic activity in the auditory

91    cortex (Coffey et al., 2017b), consistent with the relative specialization of right auditory cortex

92    for pitch and tonal processing (Zatorre and Berlin, 2001; Patterson et al., 2002; Hyde et al.,

93    2008; Albouy et al., 2013; Cha et al., 2016).

94        Despite findings that show the potential cortical contribution to FFRs, it is unclear

95    whether the relationship between auditory cortex and FFR is causal. The aim of the present

96    study was to determine such relationship. Here, transcranial direct current stimulation (tDCS)

97    was applied to alter neural excitability in the left and right auditory cortices. We examined the

98    after-effects of tDCS on speech-evoked FFR using electroencephalography (EEG). tDCS is a

99    non-invasive neuro-stimulation that modulates cortical excitability (Jacobson et al., 2012). By

100   applying direct currents over the scalp, tDCS leads to neural excitation or inhibition in

101   proximal parts of the cortex that last for up to 90 minutes post-stimulation (Nitsche and Paulus,

102   2001). Previous studies showed that applying tDCS over the right, compared to the left,

103   auditory cortex can significantly change pitch discrimination performances, supporting the

104   causal role of the right auditory cortex for pitch perception (Mathys et al., 2010; Matsushita et

105   al., 2015). However, such causality has not been established for neurophysiological signatures

106   like FFR. The present study tested the hypothesis that tDCS over the right auditory cortex

107   should change the FFR strength during monaural listening to speech syllables. We further

108   predicted that such after-effects should occur particularly along the contralateral auditory

109   pathway where participants listen to speech from the left ear.

110

# Materials and Methods

## Participants

113       Ninety participants (18-40 years old; 45 females) were recruited and completed the entire

114   experiment. Two other participants dropped out during the tDCS phase because they felt

115   uncomfortable with the skin sensation when stimulation was applied. All participants had

116   normal hearing (pure-tone audiometric thresholds <25 dB HL within frequency range of 0.25–

117    6 kHz for both ears) tested using a MAICO MA41 Audiometer (MAICO Diagnostics,

118    Germany). Participants were non-tonal language speakers, had no long-term musical training

119    and reported no history of neurological or speech/language disorders. They had not participated

120    in any brain stimulation experiments in the two weeks prior to the present experiment.

121    All participants were right-handed (Handedness Index (HI) > 40; Oldfield, 1971). They

122    were assigned at random to one of five groups, each of which received different types of tDCS

123    (detailed in *Experimental design*). HI did not differ significantly between the five groups (all *p*

124    > 0.4, uncorrected), indicating that the degree of handedness was well-matched across

125    stimulation types. The absence of HI differences across groups is important because it has been

126    argued that handedness influences functional hemispheric specialization (Carey et al., 2014;

127    Willems et al., 2014). Hence matching the HI across groups ensured that any effects of tDCS

128    were not confounded by handedness.

## Syllable stimulus for the FFR recording

130    A 120-ms-long syllable /i/ spoken by a male with a static fundamental frequency ($F_0$) at

131    136 Hz was used for the FFR recordings. The waveform and spectrum of the syllable are

132    shown as **Figure 1**. The syllable has three formants (F1, F2 and F3 at ~280, 2400 and 3100 Hz,

133    respectively). It has a stable amplitude profile across the syllable period except for the 5-ms

134    rising and falling cosine ramps applied at the onset and offset to avoid transients.
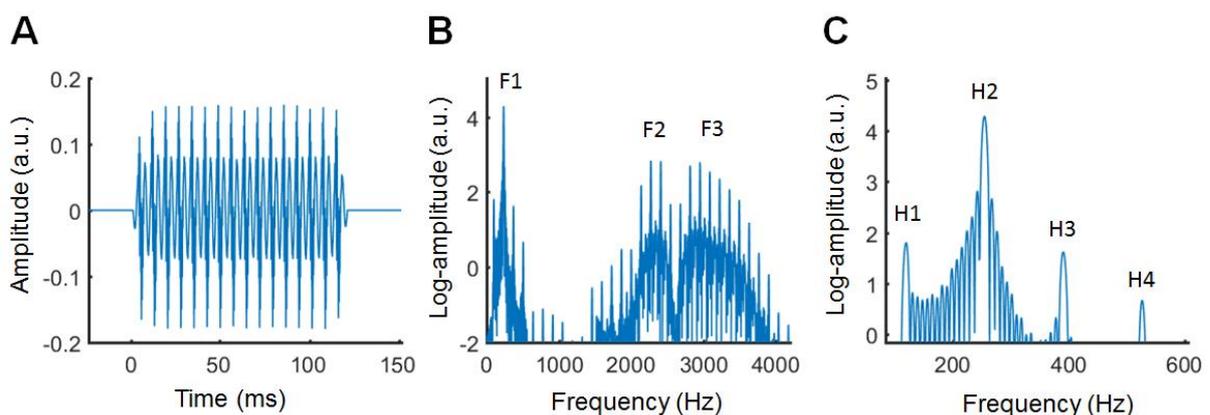


135
136   **Figure 1. The syllable stimulus for FFR recordings. (A)** Temporal waveform of the syllable

137    /i/. **(B)** Spectrum of the syllable (0–4000 Hz) showing the formant locations (F1, F2 and F3).

138    **(C)** The same spectrum as **(B)** that shows the first four harmonics with $F_0$ at 136 Hz. *N.B.*, the

139    spectrum was obtained via Fast Fourier Transform (FFT) after zero-padding the temporal

140    waveform to 1 second.

## Experimental design

The experimental procedure is summarized in **Figure 2**. FFRs were recorded pre- and post-tDCS during monaural listening to the syllable stimulus to test for any after-effects of tDCS.

### *FFR recording*

EEG were recorded over participants' scalps using an ActiveTwo system (Biosemi ActiView, The Netherlands) with sampling rate of 16,384 Hz whilst they listened to the repeatedly-presented syllable /i/ (see *Syllable stimulus for the FFR recording*) both pre- and post-tDCS. The recording site was at the vertex (Cz) localized using a standard Biosemi cap, which is the conventional site used for obtaining FFRs (Skoe and Kraus, 2010). Bilateral earlobes served as the reference and ground electrodes were CMS and DRL at the parieto-occipital sites. Electrode impedance was kept below 35 mV. The syllable stimulus was presented at ~4 times per second with inter-stimulus interval (ISI) fixed at 120 ms. The stimulus was played monaurally via electrically-shielded inserted earphone (ER-3 insert earphone, Intelligent Hearing Systems, Miami, FL) at 85 dB SL (excluding ISIs) in each ear (e.g. left-ear listening followed by right-ear listening or vice versa with order of ear presentation counterbalanced across participants). Monaural listening ensured that after-effects of ipsilateral and contralateral tDCS (relative to the listening ears) could be tested separately (see *Statistical analyses*). For each ear, there were 1,500 sweeps for the positive and 1,500 sweeps for the negative polarity presented in an intermixed order (i.e., 3,000 sweeps in total).

Participants were seated comfortably in an armchair in an electromagnetically- and sound-shielded booth. They listened passively to the stimulus sequence whilst keeping their eyes on a fixation cross in the centre of a computer screen. The 3,000 syllable sweeps in each ear were broken into six 2-minute-long blocks (500 sweeps each) with ~40 second breaks between blocks. Participants were required to keep awake and refrain from body and head movements whilst they were listening to the sounds. The FFR recording lasted for ~30 minutes for both pre- and post-tDCS. The post-tDCS recording was completed within 45 minutes post-tDCS for all participants to ensure that any after-effects of tDCS on FFRs were sustained (Nitsche and Paulus, 2001).

### *tDCS*

171        tDCS was applied over the scalp using a battery-driven direct current stimulator
172        (Magstim HDCStim, UK) with a pair of rubber-surface electrodes (5×5 cm) contained in
173        saline-soaked cotton pads. Participants were assigned at random to one of the five groups (18
174        participants (9 females) per group; single-blinded). The five groups received the following
175        different types of tDCS: (1) anodal stimulation on the left auditory cortex (AC) (Left-Anod);
176        (2) cathodal stimulation on the left AC (Left-Cathod); (3) anodal stimulation on the right AC
177        (Right-Anod); (4) cathodal stimulation on the right AC (Right-Cathod); and (5) Sham, with
178        electrode configurations randomly chosen from (1)–(4) for each participant (in this group, the
179        active electrode was put on the left AC for half of the participants and on the right AC for the
180        other half). Centre position of the active electrode was on T7/T8 (according to the 10/20 EEG
181        system) for the left/right AC. The reference electrode was placed on the forehead above the
182        eyebrow contralateral to the active electrode (see Matsushita et al., 2015; also see **Figure 2**).
183        For groups (1)–(4), tDCS was applied at 1 mA for 25 minutes with the currents ramping
184        up/down for 15 seconds at the stimulation onset/offset. Sham applied tDCS only for 30 seconds
185        in total (15 seconds ramping up and down respectively) at the onset of stimulation. This
186        created the usual sensations associated with tDCS in Sham but without actual stimulation
187        during the remainder of the run. All experimental sessions were conducted during the day time
188        (mornings or early afternoons) and all participants had enough sleep (at least 6 hrs) the night
189        before (based on self-report prior to the experiment) to ensure adequate cortical plasticity
190        triggered by tDCS (Salehinejad et al., 2019).

191        During tDCS, participants completed a pitch discrimination task while they listened to
192        sound stimuli over a loudspeaker 1 metre in front of them in the same sound-shielded booth
193        used for the FFR recordings. Three short complex tones (400 ms) were presented on each trial
194        at a calibrated level of 75 dB SL at the 1 metre position. The task was an 'ABX' task. In each
195        trial, two tones 'A' and 'B' with different fundamental frequencies ($F_0$) were played
196        consecutively followed by a third tone 'X' randomly selected from 'A' or 'B'. Participants had
197        to identify whether 'X' was the same as 'A' or 'B'. They gave their best guess when they were
198        unsure of the answer. The process followed a '2-down, 1-up' adaptive procedure, in which the
199        $F_0$ difference between 'A' and 'B' decreased by $\sqrt{2}$ times following two consecutive correct
200        trials and increased by $\sqrt{2}$ times following an incorrect trial. No feedback about response
201        accuracy was provided. Half-minute breaks were taken every 4 minutes. This task was
202        included during tDCS because tDCS preferentially modulates neural networks that are
203        currently active (Reato et al., 2010; Ranieri et al., 2012; Bikson and Rahman, 2013).

204    Concurrent tDCS and the pitch discrimination task could therefore maintain auditory cortical

205    activity during neuro-stimulation, hence maximizing the effect of tDCS on neural excitability.
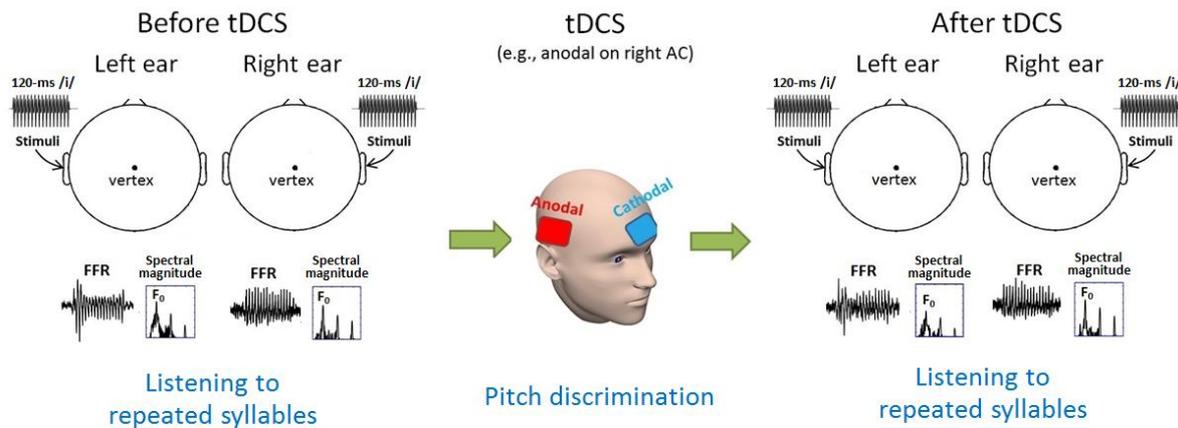


206

207    **Figure 2. Illustrations for the experiment design.** Participants first listened to a repeated

208    syllable /i/ monaurally while FFR was recorded over scalp-EEGs at Cz. tDCS was then applied

209    over the auditory cortex (AC) along with a pitch discrimination task. The same syllable

210    listening task as in the first step was finally performed following tDCS to detect any after-

211    effects of neuro-stimulation.

212

## EEG Signal processing

214    All EEG signal processing was conducted via Matlab R2017a (The Mathworks).

### Pre-processing

216    As mentioned, the FFR was captured from Cz. The EEG signals were first re-referenced

217    to the bilateral earlobes and bandpass-filtered between 90 and 4000 Hz using a $2^{nd}$-order zero-

218    phase Butterworth filter. The filtered signals were then segmented for each sweep (-50 to 150

219    ms relative to the syllable onset). Each segment was baseline-corrected by subtracting the

220    average of the pre-stimulus (-50–0 ms) period. Segments that exceeded ±25 mV were rejected

221    to minimize movement artefacts. The resultant rejection rates were < 2.5% averaged across

222    participants for all cases (pre- and post-tDCS for the five stimulation groups for both left and

223    right ear conditions).

### FFR magnitudes

225    FFRs with the positive and negative polarities ($FFR_{Pos}$ and $FFR_{Neg}$) were first obtained by

226    temporally averaging the pre-processed signals across sweeps with the respective polarities.

227    FFRs for envelopes of $F_0$ and its harmonics (i.e., periodicity; $FFR_{ENV}$) and temporal fine

228    structures (TFS; $FFR_{TFS}$) were obtained by adding and subtracting $FFR_{Pos}$ and $FFR_{Neg}$,

229    respectively (Aiken and Picton, 2008). The addition and subtraction minimized the responses

230    to TFS in $FFR_{ENV}$ and to envelopes in $FFR_{TFS}$, so that purer FFRs to envelopes and TFS were

231    obtained separately (Aiken and Picton, 2008). Spectral magnitudes of $FFR_{ENV}$ and $FFR_{TFS}$

232    were then calculated.
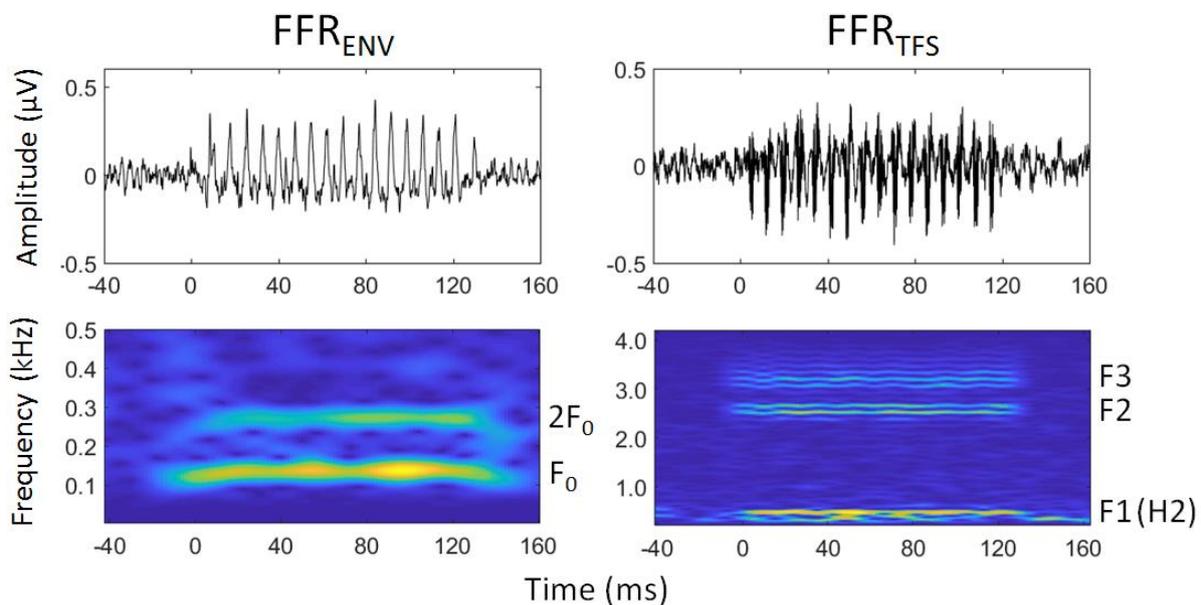


233
234    **Figure 3. A representative sample of FFR.** Sample waveforms (top panels) and the

235    corresponding spectrograms (lower panels) of $FFR_{ENV}$ (left) and $FFR_{TFS}$ (right) were obtained

236    from a single participant in the left ear listening condition before tDCS was applied. The first

237    two harmonics of $F_0$ ($F_0$ and $2F_0$) dominate the power of $FFR_{ENV}$ as indicated in the $FFR_{ENV}$

238    spectrogram (lower left). The three formants (F1, F2 and F3) in $FFR_{TFS}$ are shown and

239    indicated in the $FFR_{TFS}$ spectrogram (lower right); F1 occurs at H2 for this vowel (the 2nd

240    harmonic).

241

242    For $FFR_{ENV}$, $FFR_{ENV\_F0}$ and $FFR_{ENV\_2F0}$ ($FFR_{ENV}$ at $F_0$ and its 2nd harmonic, $2F_0$) that

243    dominate the power of $FFR_{ENV}$ (see **Figure 3** left panel) were focused on. Whereas $FFR_{ENV\_F0}$

244    and $FFR_{ENV\_2F0}$ reflect neural phase-locking to the stimulus envelope periodicity in the central

245    auditory systems, higher harmonics ($\geq 3$) of $FFR_{ENV}$ may reflect distortion products resulting

246    from non-linearities in response to acoustic stimuli on the basilar membrane (Smalt et al.,

247    2012). Whilst it is expected that $FFR_{ENV\_F0}$ plays the major role in phase-locking to speech

248    periodicity, $FFR_{ENV\_2F0}$ also makes contributions (e.g., Aiken and Picton, 2008) because of the

249    non-sinusoidal characteristics of speech periodicity (Holmberg et al., 1988; also see

250    discussions in Smalt et al., 2012). The procedure for measuring the magnitudes of $FFR_{ENV\_F0}$

251    and $FFR_{ENV\_2F0}$ was as follows: a set of 120 ms (same length as the stimulus syllable) sliding

252    windows (1 ms per step), each with a 5-ms rising/falling cosine ramp at the onset/offset, was

253    applied to the $FFR_{ENV}$ waveform. As $FFR_{ENV}$ occurs at the auditory brainstem (Chandrasekaran

254    and Kraus, 2010; Bidelman, 2015, 2018) and/or primary auditory cortex (Coffey et al., 2016),

255    the neural transmission delays were set at 5–20 ms. Onsets of the windows were therefore set

256    at 6–21 ms (allowing for an additional ~1 ms sound transmission through the plastic tube of the

257    earphone to the cochlea) after the syllable onset. The windowed $FFR_{ENV}$ waveform in each step

258    was then zero-padded to 1 second to allow for a frequency resolution of 1 Hz and the log-

259    transformed FFT-powers ($10*\log_{10}[power]$) centred at $F_0$ and $2F_0$ were measured (averaged

260    across $136 \pm 2$ Hz and $272 \pm 2$ Hz, respectively). Finally, the $FFR_{ENV\_F0}$ and $FFR_{ENV\_2F0}$

261    magnitudes were taken as the powers at the optimal neural delays (i.e., when powers are

262    maximal across all steps for $F_0$ and $2F_0$, respectively).

263       For $FFR_{TFS}$, $FFR_{TFS\_H2}$ and $FFR_{TFS\_F2F3}$ ($FFR_{TFS}$ at the $2^{nd}$ harmonic that represents F1

264    for this vowel, and at F2 and F3, respectively; see **Figure 4.3** right panel) were focused on.

265    $FFR_{TFS\_H2}$ reflects FFR to TFS at the resolved-harmonic region while $FFR_{TFS\_F2F3}$ reflects FFR

266    to TFS at the unresolved-harmonic region. The same procedure used when measuring

267    magnitudes of $FFR_{ENV\_F0}$ and $FFR_{ENV\_2F0}$ was followed, except that: (1) the procedure was

268    applied on $FFR_{TFS}$ at H2 (for $FFR_{TFS\_H2}$) and at H16–H27 (the $16^{th}$ to $27^{th}$ harmonics

269    corresponding to the range of F2 and F3 for $FFR_{TFS\_F2F3}$; the final magnitude was taken as the

270    mean magnitude across all harmonics in this range); (2) the neural delays during analyses were

271    set at 1–6 ms (0–5 ms delays allowing an additional 1 ms sound transmission through the

272    plastic tube of the earphone) as $FFR_{TFS}$ arises at earlier stages of auditory processing in the

273    periphery (Aiken and Picton, 2008).

274       Because of the different neural origins of $FFR_{ENV}$ (brainstem/auditory cortex) and

275    $FFR_{TFS}$ (periphery), the present study thus allows us to confirm whether tDCS applied to

276    auditory cortex affects FFR that arise at different levels of the auditory systems.

277    **Statistical analyses**

278    Before testing the after-effects of tDCS, analyses were first conducted to check whether

279    baseline (pre-tDCS) characteristics were matched across stimulation. ANOVAs were

280    conducted using the baseline magnitudes and optimal neural delays of FFRs as dependent

281    variables, Stimulation (Left-Anod, Left-Cathod, Right-Anod, Right-Cathod and Sham) and Ear

282    (left vs. right) as independent variables. Post-hoc analyses were conducted following

283    significant interactions or main effects.

284    After-effects of tDCS (differences in FFR magnitudes between post- and pre-tDCS) were

285    tested using linear mixed-effect regressions. These were conducted using after-effects as

286    dependent variables, Stimulation and Ear as fixed-effect factors and Participant as the random-

287    effect factor. Post-hoc analyses were conducted following significant interactions or main

288    effects.

289    Furthermore, regardless of whether interaction effects occurred between Stimulation and

290    Ear, planned comparisons for the after-effects were conducted between different stimulation

291    types in the left and right ear conditions, respectively. This was because collapsing the left and

292    right ears would smear the distinctions between any after-effects along the contralateral

293    pathway (ears with tDCS on the opposite side) and those along the ipsilateral pathway (ears

294    with tDCS on the same side), which was one of the aspects addressed in the present study. As

295    multiple comparisons were conducted for each ear (5 stimulation types leading to 10

296    comparisons), the critical α value for detecting significance was adjusted at 0.005. It was

297    predicted that, compared to Sham, significantly greater after-effects of tDCS over the right

298    auditory cortex (Right-Anod and Right-Cathod), but not the left auditory cortex (Left-Anod or

299    Left-Cathod), should be found, consistent with the current hypothesis that the right auditory

300    cortex makes specific contributions to FFR.

301    FFR magnitudes were magnitudes of $FFR_{ENV}$ ($FFR_{ENV\_F0}$ and $FFR_{ENV\_2F0}$) and $FFR_{TFS}$

302    ($FFR_{TFS\_H2}$ and $FFR_{TFS\_F2F3}$) (see *EEG signal processing*). For $FFR_{ENV}$, the present study

303    combined the magnitudes of $FFR_{ENV\_F0}$ and $FFR_{ENV\_2F0}$, rather than use them as separate

304    dependent variables. The reason was that, it was observed that the summed $FFR_{ENV\_F0}$ and

305    $FFR_{ENV\_2F0}$ magnitude yielded greater effect sizes during planned comparisons where statistical

306    significance ($p < 0.05$, uncorrected) was detected using $FFR_{ENV\_F0}$ or $FFR_{ENV\_2F0}$ magnitude

307    alone: Cohen's $d$ = 0.752 and 1.001 for $FFR_{ENV\_F0}$ and for the summed $FFR_{ENV\_F0}$ and

308    $FFR_{ENV\_2F0}$ magnitude, respectively, when Right-Anod was compared with Sham in the left ear

309    listening condition; Cohen's $d$ = 0.934 and 1.140 for $FFR_{ENV\_F0}$ and for combined $FFR_{ENV\_F0}$

310   and $FFR_{ENV\_2F0}$ magnitude, respectively, when Right-Cathod was compared with Sham in the

311   left ear listening condition (see *Results* for further details).

312

# Results

## Baseline characteristics

315   **Table 1** and **2** shows the baseline magnitudes and neural delays for $FFR_{ENV}$, $FFR_{TFS\_H2}$

316   and $FFR_{TFS\_F2F3}$ in both the left and right ear conditions. ANOVAs were conducted for baseline

317   magnitudes and optimal neural delays of $FFR_{ENV}$, $FFR_{TFS\_H2}$ and $FFR_{TFS\_F2F3}$.

318   For $FFR_{ENV}$, a significant main effect of Ear was found for the magnitude ($F(1, 85) =$

319   $12.318, p < 0.001$; greater magnitude in the left than in the right ear condition) but not for the

320   neural delay ($F(1, 85) = 0.055, p = 0.815$); no main effects of Stimulation (magnitude: $F(4, 85)$

321   $= 0.932, p = 0.450$; neural delay: $F(4, 85) = 0.799, p = 0.529$) or [Stimulation $\times$ Ear]

322   interactions were found (magnitude: $F(4, 85) = 0.541, p = 0.706$; neural delay: $F(4, 85) =$

323   $0.046, p = 0.996$). Furthermore, no significant differences were found between any stimulation

324   type in either ear condition (magnitude: all $p > 0.07$; neural delay: all $p > 0.1$). **Figure 4**

325   illustrates the comparison of baseline magnitudes for $FFR_{ENV}$ between the left and right ear

326   conditions after collapsing across stimulation types (due to the significant main effect of Ear

327   but no main effect of Stimulation).

328   For $FFR_{TFS\_H2}$, there were no significant main effects of Stimulation (magnitude: $F(4, 85)$

329   $= 0.692, p = 0.600$; neural delay: $F(4, 85) = 1.421, p = 0.234$) or Ear (magnitude: $F(1, 85) =$

330   $3.483, p = 0.065$; neural delay: $F(1, 85) = 1.842, p = 0.178$), or [Stimulation $\times$ Ear] interactions

331   (magnitude: $F(4, 85) = 0.744, p = 0.565$; neural delay: $F(4, 85) = 0.587, p = 0.673$). No

332   significant differences were found between any stimulation type in either ear condition

333   (magnitude: all $p > 0.1$; neural delay: all $p > 0.05$).

334   For $FFR_{TFS\_F2F3}$, significant main effects of Stimulation ($F(4, 85) = 40.872, p < 0.001$)

335   and Ear ($F(1, 85) = 4.225, p = 0.002$; greater in the right than the left ear condition) were found

336   for the magnitude, but not for the neural delay (Stimulation: $F(4, 85) = 1.504; p = 0.208$; Ear:

337   $F(1, 85) = 0.324, p = 0.571$). A significant [Stimulation $\times$ Ear] interaction was found for the

338   neural delay ($F(4, 85) = 2.549, p = 0.045$), but not for the magnitude ($F(4, 85) = 1.763, p =$

12

339  0.144). Post-hoc analyses found significant differences in magnitudes between several
340  stimulation types (collapsing the left and right ears: Left-Anod vs. Right-Anod, t(34) = -2.110,
341  $p$ = 0.042; Left-Anod vs. Sham, t(34) = -2.713, $p$ = 0.010; Left-Cathod vs. Right-Anod, t(34) =
342  -2.796, $p$ = 0.008; Left-Cathod vs. Right-Cathod, t(34) = -2.566, $p$ = 0.015; Left-Cathod vs.
343  Sham, t(34) = -3.498, $p$ = 0.001). Significant differences were found between stimulation types
344  for the neural delay in both the left ear (Left-Anod vs. Right-Cathod, t(34) = -2.703, $p$ = 0.011)
345  and the right ear condition (Right-Anod vs. Right-Cathod, t(34) = 2.279, $p$ = 0.029; Left-Anod
346  vs. Right-Anod, t(34) = -2.240, $p$ = 0.032; Right-Anod vs. Sham, t(34) = 2.629, $p$ = 0.013). All
347  $p$-values here are reported without correction.

348       The results thus indicate that the baseline characteristics of $FFR_{ENV}$ and $FFR_{TFS\_H2}$, but
349  not $FFR_{TFS\_F2F3}$, were well matched across stimulation types. As such, although after-effects
350  were tested for all three FFR signatures, $FFR_{ENV}$ and $FFR_{TFS\_H2}$ are focused on. In addition, the
351  main effects of Ear for $FFR_{ENV}$ and $FFR_{TFS\_F2F3}$ magnitudes may reflect the laterality of speech
352  encoding at the subcortical (Chandrasekaran and Kraus, 2010; Bidelman, 2015, 2018) and/or
353  cortical levels (Coffey et al., 2016, 2017b), which will be discussed further (see *Discussion*).

354

355  **Table 1.** Baseline magnitudes (standard deviations shown in the brackets; in *dB*) for $FFR_{ENV}$,
356  $FFR_{TFS\_H2}$ and $FFR_{TFS\_F2F3}$ across stimulation types in the left and right ear conditions.

| FFRs | Ear | Left-Anod | Left-Cathod | Right-Anod | Right-Cathod | Sham |
|---|---|---|---|---|---|---|
| $FFR_{ENV}$ | Left | 76.28 (5.27) | 78.84 (7.03) | 76.05 (6.96) | 76.24 (8.56) | 73.45 (10.05) |
|  | Right | 75.05 (5.79) | 75.42 (4.72) | 72.82 (6.62) | 74.24 (7.91) | 72.17 (10.92) |
| $FFR_{TFS\_H2}$ | Left | 30.35 (5.70) | 30.70 (7.71) | 32.52 (7.12) | 31.68 (6.24) | 33.37 (6.86) |
|  | Right | 32.71 (3.88) | 30.63 (6.98) | 32.59 (7.97) | 33.40 (7.51) | 34.36 (5.66) |
| $FFR_{TFS\_F2F3}$ | Left | 15.31 (7.26) | 13.21 (7.24) | 19.45 (7.16) | 20.14 (6.58) | 20.46 (5.75) |
|  | Right | 17.13 (7.07) | 16.28 (6.58) | 22.97 (7.57) | 20.90 (7.82) | 23.58 (6.09) |

357

358  **Table 2.** Baseline neural delays (standard deviations shown in the brackets; in *ms*) for $FFR_{ENV}$,
359  $FFR_{TFS\_H2}$ and $FFR_{TFS\_F2F3}$ across stimulation types in the left and right ear conditions.

13

| FFRs | Ear | Left-Anod | Left-Cathod | Right-Anod | Right-Cathod | Sham |
|------|-----|-----------|-------------|------------|--------------|------|
| $FFR_{ENV}$ | Left | 8.75 (2.45) | 9.42 (2.44) | 9.67 (2.70) | 8.56 (2.81) | 8.81 (2.71) |
| | Right | 8.78 (2.02) | 9.47 (3.49) | 9.50 (3.25) | 8.58 (1.69) | 9.08 (2.33) |
| $FFR_{TFS\_H2}$ | Left | 3.50 (2.28) | 4.50 (1.82) | 3.50 (1.82) | 3.67 (2.06) | 4.28 (1.60) |
| | Right | 3.61 (2.30) | 4.94 (1.59) | 4.44 (1.95) | 4.11 (2.00) | 4.06 (1.92) |
| $FFR_{TFS\_F2F3}$ | Left | 2.90 (0.36) | 3.04 (0.27) | 3.03 (0.44) | 3.20 (0.31) | 3.05 (0.53) |
| | Right | 2.93 (0.48) | 3.03 (0.48) | 3.28 (0.47) | 2.97 (0.34) | 2.87 (0.48) |

360



361
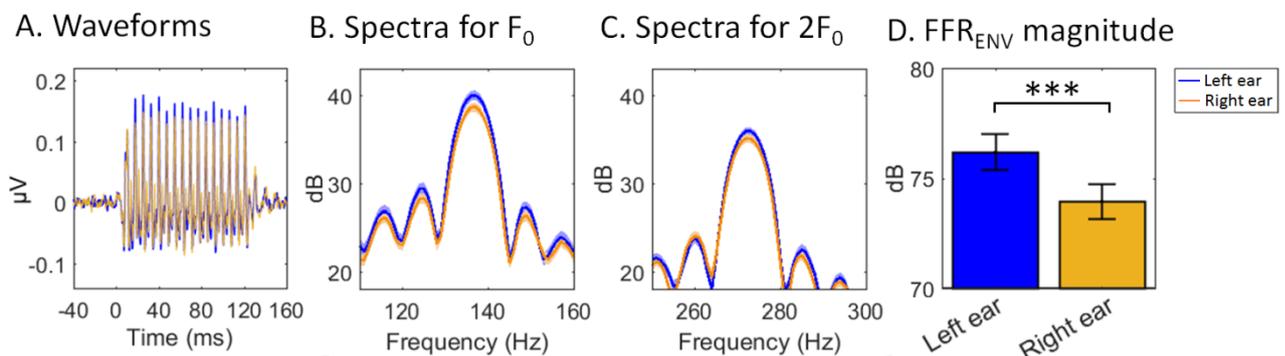
**Figure 4. Comparison of baseline magnitude for $FFR_{ENV}$ between the left and the right ear conditions.** The comparison was conducted by collapsing the stimulation types following the ANOVA results which showed a significant main effect of Ear, but no significant main effect of Stimulation or [Stimulation × Ear] interaction for the baseline $FFR_{ENV}$ magnitude. The left and the right ear conditions are indicated as *blue* and *orange*, respectively. **(A)** Waveforms of $FFR_{ENV}$ averaged across stimulation types. **(B)(C)** FFT-power spectra averaged across stimulation types, obtained using the individual optimal neural delays for **(B)** $FFR_{ENV\_F0}$ (showing 110–160 Hz peaking at $F_0$ of 136 Hz) and **(C)** $FFR_{ENV\_2F0}$ (showing 250–300 Hz peaking at $2F_0$ 272 Hz) (shaded areas in the spectra cover the ranges of ±1 standard errors (SEs)). **(D)** $FFR_{ENV}$ magnitude (summed magnitude of $FFR_{ENV\_F0}$ and $FFR_{ENV\_2F0}$). Significant greater $FFR_{ENV}$ magnitude was found in the left than in the right ear condition (***$p < 0.001$, uncorrected). Error bars indicate the SEs.

## After-effects on $FFR_{ENV}$

$FFR_{ENV}$ magnitude refers to the summed $FFR_{ENV\_F0}$ and $FFR_{ENV\_2F0}$ magnitudes (see Statistical analyses). **Figure 5** shows the waveforms and FFT-power spectra for $FFR_{ENV}$ across

14

377    participants. Linear mixed-effect regression showed a significant main effect of Stimulation

378    ($F(4, 85) = 2.549$, $p = 0.045$). No main effect of Ear ($F(1, 85) = 0.784$, $p = 0.378$) or

379    [Stimulation $\times$ Ear] interaction ($F(4, 85) = 1.309$, $p = 0.273$) was found. Post-hoc independent-

380    sample t-tests were thus conducted between different stimulation types following the main

381    effect of Stimulation (collapsing the left and right ear due to the lack of [Stimulation $\times$ Ear]

382    interaction). After-effects of tDCS over the right AC were significantly lower than that of

383    Sham (Right-Anod vs. Sham, $t(34) = -2.569$, $p = 0.015$ (uncorrected), Cohen's $d = 0.856$;

384    Right-Cathod vs. Sham, $t(34) = -2.219$, $p = 0.033$ (uncorrected), Cohen's $d = 0.740$) (**Figure**

385    **6**).
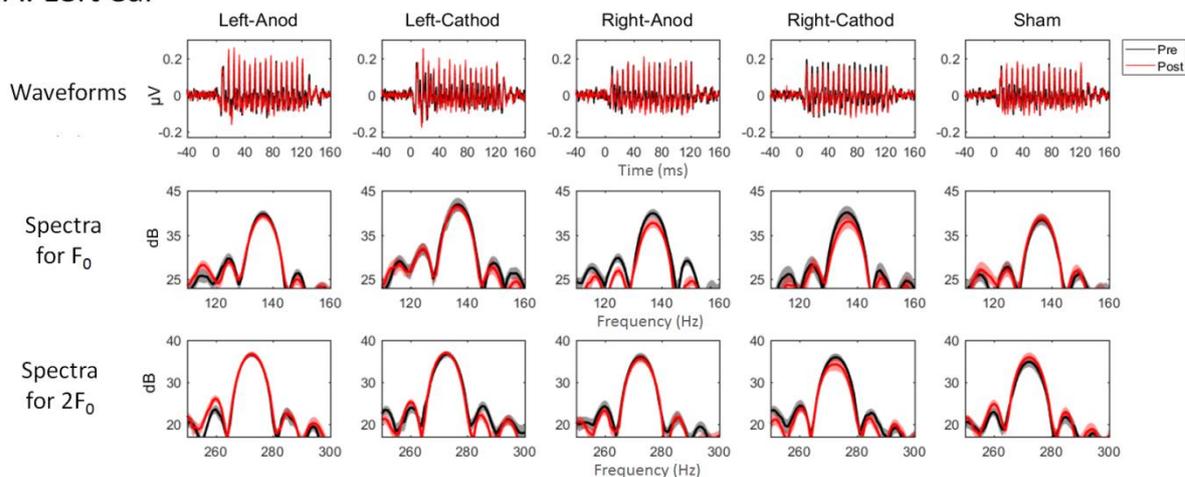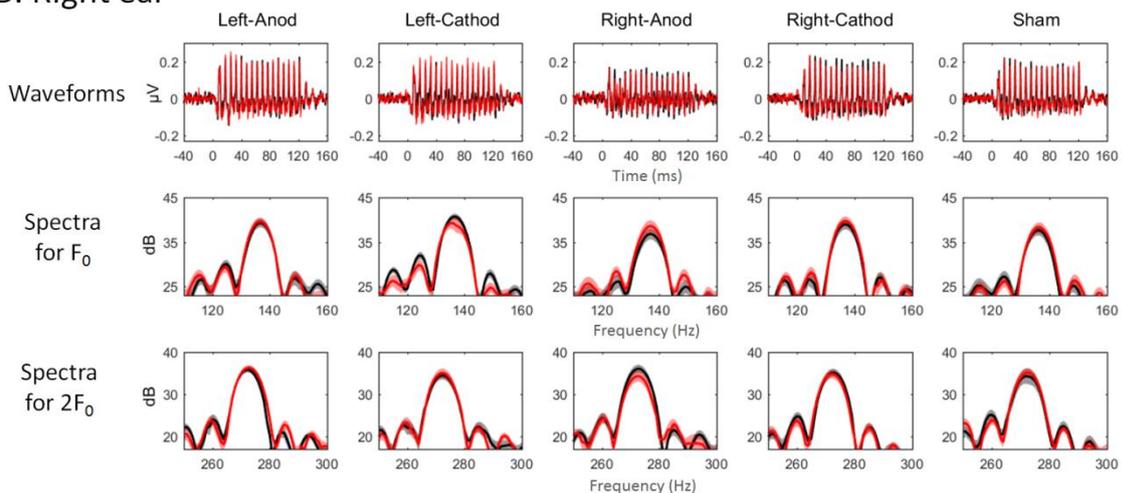


386
387    **Figure 5. Waveforms and power spectra for FFR$_{ENV}$ averaged across participants**. **(A)** and

388    **(B)** show the waveforms and FFT-power spectra in the left and right ear condition,

389    respectively. Pre- and post-tDCS were indicated as *black* and *red*, respectively (shaded areas

390    in the spectra cover the ranges of $\pm1$ SEs from the means). From left to right are different

391    stimulation types (Left-Anod, Left-Cathod, Right-Anod, Right-Cathod and Sham). *Upper*

392    panels: waveforms of $FFR_{ENV}$; *mid* and *lower* panels: power spectra obtained using the

393    individual optimal neural delays for $FFR_{ENV\_F0}$ (*mid*; showing 110–160 Hz peaking at $F_0$ of 136

394    Hz) and $FFR_{ENV\_2F0}$ (l*ower*; showing 250–300 Hz peaking at $2F_0$ of 272 Hz).
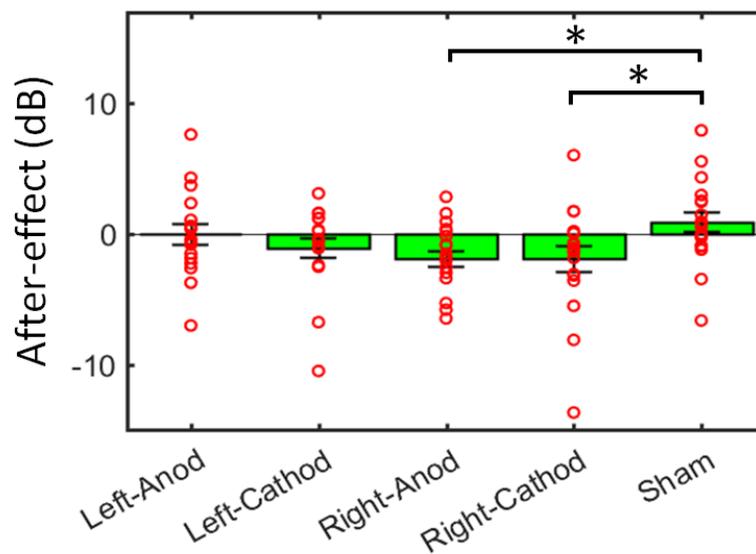


395

396    **Figure 6. After-effects of tDCS on $FFR_{ENV}$ magnitudes comparing across stimulation**

397    **types after collapsing the left and right ears**. Collapsing the left and right ears was

398    conducted following the ANOVA results which showed a significant main effect of

399    Stimulation but no significant main effect of Ear or [Stimulation $\times$ Ear] interaction. Red circles

400    indicate individual data for the corresponding stimulation types (Left-Anod, Left-Cathod,

401    Right-Anod, Right-Cathod and Sham). Post-hoc paired comparisons showed significant

402    differences between tDCS over the right AC (Right-Anod and Right-Cathod) and Sham (*$p <$

403    0.05, uncorrected). Error bars indicate the SEs.

404

405        Planned comparisons between different stimulation types were subsequently conducted

406    for the left and right ear listening conditions to determine whether tDCS has effects along the

407    contralateral or ipsilateral pathway. The critical $\alpha$ value for detecting significance was adjusted

408    to 0.005 (there were 10 pairs of comparisons in each ear condition). The results are illustrated

409    in **Figure 7** (upper panels). In the left ear condition, significant differences were found between

410    tDCS over the right AC and Sham (Right-Anod vs. Sham, $t(34) = -3.024$, $p < 0.005$, Cohen's *d*

16

411    = 1.001; Right-Cathod vs. Sham, t(34) = -3.420, $p$ = 0.002, Cohen's $d$ = 1.140). No significant

412    effects were found for any other comparison (all $p > 0.2$). In the right ear condition, no

413    significant effects were found for any pair of comparison (all $p > 0.2$). All $p$-values shown here

414    are reported without correction.
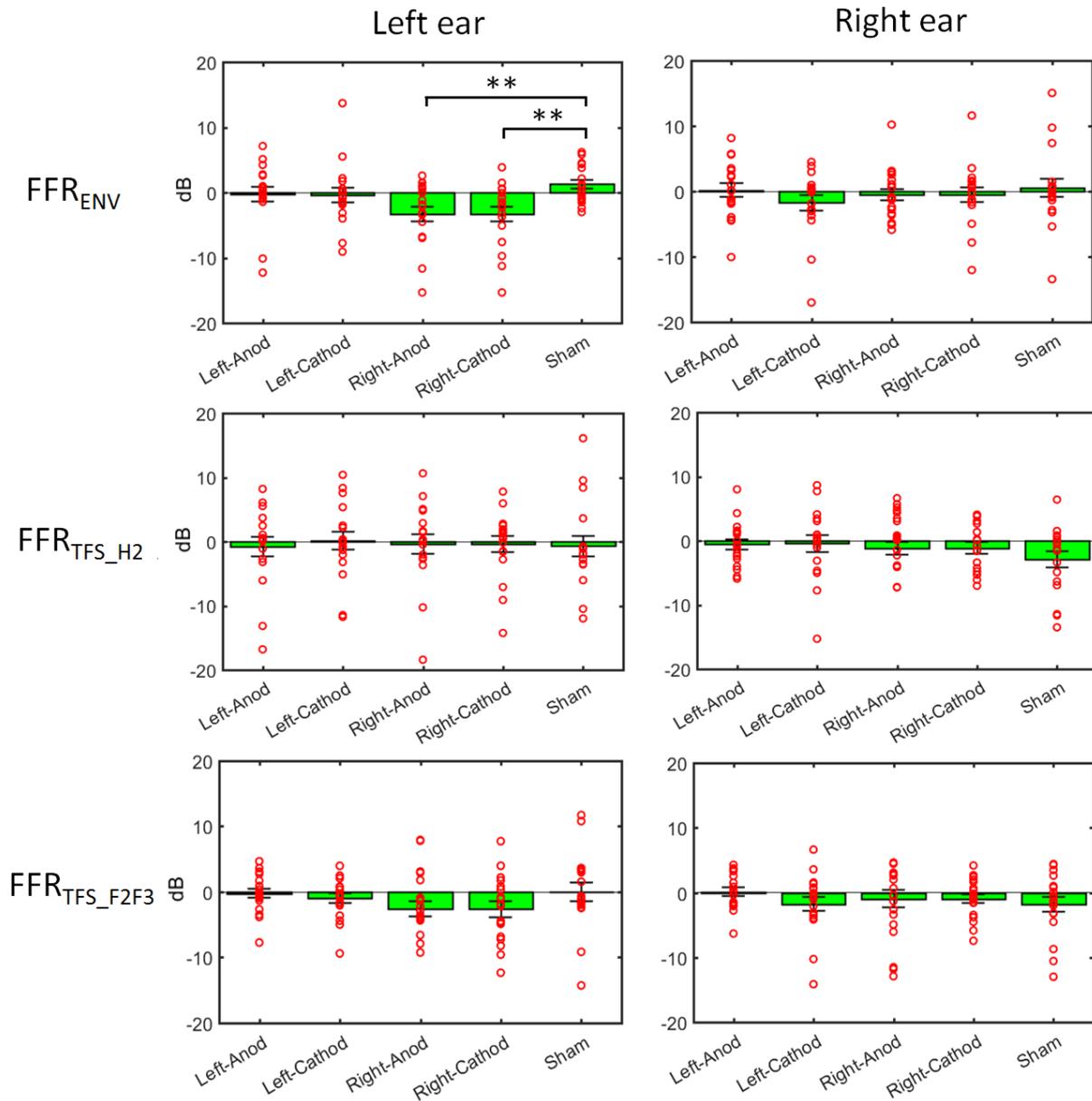


415
416 **Figure 7. After-effects of tDCS on FFR magnitudes.** Upper, mid and lower panels indicate

417    the after-effects on magnitudes of $FFR_{ENV}$, $FFR_{TFS\_H2}$ and $FFR_{TFS\_F2F3}$, respectively. Planned

418    comparisons were conducted between different stimulation types in both the left and right ear

419    conditions, with the critical α value set at 0.005 according to multiple comparisons. Significant

420    differences were found between tDCS over the right auditory cortex (Right-Anod and Right-

421    Cathod) and Sham in the left ear condition for $FFR_{ENV}$. (**$p < 0.005$, uncorrected; i.e., $p <$

422    0.05 after correction according to multiple comparisons) Red circles indicate individual data

423    for the corresponding stimulation types. Error bars indicate the SEs.

424

## After-effects on FFR$_{TFS}$

426      Equivalent analyses to those conducted for the FFR$_{ENV}$ magnitude were conducted for

427    the magnitudes of FFR$_{TFS\_H2}$ and FFR$_{TFS\_F2F3}$. The linear mixed-effect regressions did not show

428    significant main effects of Stimulation (FFR$_{TFS\_H2}$: $F(4, 85) = 0.528$, $p = 0.715$; FFR$_{TFS\_F2F3}$:

429    $F(4, 85) = 0.613$, $p = 0.655$) or Ear (FFR$_{TFS\_H2}$: $F(1, 85) = 0.496$, $p = 0.467$; FFR$_{TFS\_F2F3}$: $F(1,$

430    $85) = 0.213$, $p = 0.646$), or significant [Stimulation $\times$ Ear] interactions (FFR$_{TFS\_H2}$: $F(4, 85) =$

431    $0.530$, $p = 0.714$; FFR$_{TFS\_F2F3}$: $F(4, 85) = 1.189$, $p = 0.322$).

432      Planned comparisons did not find significant after-effects between different stimulation

433    types in the left or right ear condition (FFR$_{TFS\_H2}$: all $p > 0.6$ in the left ear condition and all $p >$

434    $0.1$ in the right ear condition; FFR$_{TFS\_F2F3}$: all $p > 0.09$ in the left ear condition and all $p > 0.1$

435    in the right ear condition; see **Figure 7**, mid and lower panels). All $p$-values are reported

436    without correction.

437

# Discussion

439      The current study used a combined tDCS and EEG approach to test for a causal

440    contribution of auditory cortex to speech-evoked FFR in healthy right-handed participants. The

441    left and right auditory cortices were neuro-stimulated in different groups of participants and the

442    after-effects of tDCS on the FFR were examined during monaural listening to a repeated

443    speech syllable. The results showed that tDCS, both anodal and cathodal, over the right

444    auditory cortex, generated significantly greater after-effects on FFR$_{ENV}$ magnitude compared to

445    sham stimulation. Specifically, such effects were present only in the left ear listening

446    condition, indicating that the changes in processing of speech periodicity information occur

447    along the contralateral pathway (i.e., from the left ear to the right auditory cortex). The results

448    thus agree with previous studies that have shown a close relation between the right auditory

449    cortex and FFR (Coffey et al., 2016, 2017a, 2017b; Hartmann and Weisz, 2019) and provide

450    the first evidence for a causal relationship.

## Laterality for FFR$_{ENV}$ at the baseline

Ear laterality for the baseline FFR$_{ENV}$ and FFR$_{TFS\_F2F3}$ magnitudes were found (see *Baseline characteristics*). The discussion here focuses on FFR$_{ENV}$ alone due to the significant main effect of Stimulation for the baseline FFR$_{TFS\_F2F3}$ magnitude (which means that the baseline was not well matched across stimulation types) and lack of a significant after-effect of tDCS on FFR$_{TFS\_F2F3}$ magnitude.

The present study found that baseline FFR$_{ENV}$ had significantly greater magnitude in the left than in the right ear condition, supporting the lateralization of speech periodicity encoding along the contralateral auditory pathway from the left ear to the right auditory cortex. This echoes the previous findings that showed the right-hemispheric lateralization of the classic 40 Hz auditory steady-state response (ASSR) (Ross et al., 2005; Luke et al., 2017). Right lateralization was also found in ASSR at 80 Hz (Vanvooren et al., 2014). ASSRs are phase-locked responses to amplitude-modulated tones/noise and both ASSRs and FFR$_{ENV}$ are envelope-following responses (Dimitrijevic et al., 2004). Whilst the 40 Hz ASSR has its main generator at the cortical level (Herdman et al., 2002; Ross et al., 2002, 2005), prominent activities occur at the brainstem level for the 80 Hz ASSR (Herdman et al., 2002) and speech-evoked FFR$_{ENV}$ (Chandrasekaran and Kraus, 2010; Bidelman, 2015, 2018; this can also be seen in the present study where average optimal neural delays were between 5 and 10 ms, see **Table 2**). Recent studies, however, have shown that FFR has additional sources in the auditory cortex (Coffey et al., 2016, 2017a; Hartmann and Weisz, 2019). It is thus not clear whether the observed laterality of FFR$_{ENV}$ in the present study occurs at the subcortical or cortical level or, more equivocally, whether auditory cortex contributes to this laterality. As such, the current combined tDCS and EEG approach showed how altering neural excitability of auditory cortex in the left or right hemisphere can lead to changes in FFR which therefore provides confirmatory evidence for a causal cortical contribution.

## Causal role of the right auditory cortex for FFR$_{ENV}$

After-effects found for FFR$_{ENV}$ but not FFR$_{TFS}$ indicate that tDCS had impacts on the responses at the subcortical and/or cortical levels above the auditory periphery. The findings thus argue for a causal role of the right auditory cortex in processing speech periodicity information along the contralateral pathway in the central auditory systems.

19

481    The present study thus advances our understanding of the relationship between FFR and
482    pitch processing in the right auditory cortex. Previous studies have shown that FFR is closely
483    related to pitch perception. FFR strength can be enhanced by both short-term perceptual
484    training of pitch discrimination (Carcagno and Plack, 2011) as well as long-term musical
485    experience (Musacchia et al., 2007; Wong et al., 2007; Strait et al., 2009; Bidelman et al.,
486    2011). Furthermore, FFR has been used as an index of neural fidelity of linguistic pitch and the
487    fidelity is greater in tonal language than in non-tonal language speakers (Krishnan et al., 2004,
488    2005, 2009). Despite this, however, rather than reflecting the result of pitch extraction, FFR
489    has been suggested to reflect subcortical responses to monaural temporal information (e.g.,
490    periodicity cues) that are important for extracting pitch of complex sounds (i.e., 'pitch-bearing'
491    information; Gockel et al., 2011). On the other hand, the process of pitch extraction itself takes
492    place in the auditory cortex (Penagos et al., 2004; Bendor and Wang, 2005; Puschmann et al.,
493    2010) with a right hemispheric specialization (Zatorre and Berlin, 2001; Patterson et al., 2002;
494    Hyde et al., 2008; Mathys et al., 2010; Albouy et al., 2013). In this respect, the current after-
495    effects of tDCS may reflect a top-down corticofugal modulation process in which the right
496    auditory cortex affects the processing of pitch-bearing information that occurs at the
497    subcortical level. Alternatively, although EEG mainly captures FFR signals originating from
498    the brainstem (Bidelman, 2015, 2018), cortical sources have been found dominated in the right
499    hemisphere (Coffey et al., 2016; 2017a). It therefore cannot be excluded that tDCS may affect
500    the FFR magnitude directly at the cortical level. It is noteworthy that the current finding could
501    not disentangle whether the effects emerge at the subcortical or cortical level, or both.

502    Also, stronger evidence would be provided for the specific contributions of the right
503    auditory cortex to FFR if significant differences in after-effects were further found between
504    tDCS over the right and the left auditory cortex. However, the present results did not show
505    such differences. A possible explanation is that tDCS not only alters excitability of regions in
506    which electrodes are located but can yield widespread changes across the brain (see a review:
507    Filmer et al., 2014). This could be due to the diffuse nature of the tDCS where currents do not
508    only flow between electrodes, but also spread widely through various other regions (Faria et
509    al., 2011; Bai et al., 2014; Unal and Bikson, 2018). tDCS also changes functional connectivity
510    (Sehm et al., 2012; Kunze et al., 2016) by which interactions of auditory cortices between the
511    two hemispheres may be further activated. Therefore, tDCS over the left auditory cortex could
512    also cause some changes in the right side that yield similar (but smaller) after-effects as direct
513    stimulation over the right auditory cortex.

20

## Neurophysiological consequences of tDCS

An intriguing finding of the present study is that anodal and cathodal tDCS over the right auditory cortex resulted in the same direction of changes, both causing decreases in $FFR_{ENV}$ magnitude compared to sham. Conventionally, anodal and cathodal stimulations reflect depolarization and hyperpolarization of neurons, respectively, which should lead to opposite directions of after-effects (Jacobson et al., 2012). However, it is not unusual that tDCS has polarity-independent effects due to the underlying complexity of its neurophysiological consequences. For example, several studies have shown that anodal and cathodal tDCS have the same effects on excitability of motor cortex (Antal et al., 2007), motor learning (de Xivry et al., 2011), cerebellar functions for working memory (Ferrucci et al., 2008) and visuomotor learning (Shah et al., 2013). The first possible explanation would be the non-linear effects of tDCS depending on the current density. It has been shown that cathodal tDCS with an electrode size of 35 cm$^2$ can lead to inhibition in the motor cortex at 1 mA but excitation at 2 mA (Batsikadze et al., 2013). The present study used a current intensity at 1 mA but with smaller electrode size (25 cm$^2$; hence greater current density). It could be that this current density through the auditory cortex would lead to non-linear effects as resulted in the motor cortex. Second, it is possible that similar changes in concentrations of relevant neurotransmitters are caused by anodal and cathodal tDCS. It was found that with 1 mA currents, anodal tDCS causes decreases in GABA concentration that lead to cortical excitation; cathodal tDCS also causes decreases in GABA, but with greater concurrent decreases in glutamate that lead to cortical inhibition (Stagg et al., 2009). It is possible that GABA concentrations, which decrease following both anodal and cathodal tDCS, play an important role for changes in $FFR_{ENV}$ magnitude.

## Conclusion

The current results validate the previous findings that the right auditory cortex makes significant contributions to speech-evoked FFR (Coffey et al., 2016, 2017a, 2017b; Hartmann and Weisz, 2019) by establishing a causal relationship between the two. To our knowledge, this is the first evidence for this causality and it could be essential due to the fundamental and clinical importance of the FFR. Thus, these findings should advance our understanding of how speech periodicity and pitch information are processed along the central auditory pathways in the human brain. Future research is needed to further clarify where exactly this causality emerges, i.e., to disentangle whether the effects are realized through top-down corticofugal

546 modulations on the subcortical level, or modulations directly in the cortex. Moreover, it will be

547 worthwhile to further investigate how changes in concentrations of neurotransmitters by neuro-

548 stimulation relate to this causality, which can help us better understand the underlying

549 mechanisms of the cortical contributions to FFR.

550

# References

552 Aiken SJ, Picton TW (2008) Envelope and spectral frequency-following responses to vowel

553     sounds. Hearing Research 245:35-47.

554 Albouy P, Mattout J, Bouet R, Maby E, Sanchez G, Aguera PE, Daligault S, Delpuech C,

555     Bertrand O, Caclin A, Tillmann B (2013) Impaired pitch perception and memory in

556     congenital amusia: the deficit starts in the auditory cortex. Brain 136(5):1639-1661.

557 Anderson S, Parbery-Clark A, Yi HG, Kraus N (2011) A neural basis of speech-in-noise

558     perception in older adults. Ear and Hearing 32(6):750.

559 Anderson S, Parbery-Clark A, White-Schwoch T, Kraus N (2012) Aging affects neural

560     precision of speech encoding. Journal of Neuroscience 32(41):14156-14164.

561 Antal A, Terney D, Poreisz C, Paulus W (2007) Towards unravelling task‐related

562     modulations of neuroplastic changes induced in the human motor cortex. European

563     Journal of Neuroscience 26(9):2687-2691.

564 Bai S, Dokos S, Ho KA, Loo C (2014) A computational modelling study of transcranial direct

565     current stimulation montages used in depression. NeuroImage 87:332-344.

566 Banai K, Abrams D, Kraus N (2007) Sensory-based learning disability: Insights from

567     brainstem processing of speech sounds. International Journal of Audiology 46(9):524-

568     532.

569 Batsikadze G, Moliadze V, Paulus W, Kuo MF, Nitsche MA (2013) Partially non‐linear

570     stimulation intensity‐dependent effects of direct current stimulation on motor cortex

571     excitability in humans. The Journal of Physiology 591(7):1987-2000.

572 Bendor D, Wang X (2005) The neuronal representation of pitch in primate auditory

573     cortex. Nature 436(7054):1161-1165.

574 Bidelman GM, Krishnan A, Gandour JT (2011) Enhanced brainstem encoding predicts

575     musicians' perceptual advantages with pitch. European Journal of

576     Neuroscience 33(3):530-538.

577    Bidelman GM (2015) Multichannel recordings of the human brainstem frequency-following
578         response: scalp topography, source generators, and distinctions from the transient
579         ABR. Hearing Research 323:68-80.

580    Bidelman GM (2018) Subcortical sources dominate the neuroelectric auditory frequency-
581         following response to speech. NeuroImage 175:56-69.

582    Bikson M, Rahman A (2013) Origins of specificity during tDCS: anatomical, activity-
583         selective, and input-bias mechanisms. Frontiers in Human Neuroscience 7:688.

584    Carcagno S, Plack CJ (2011) Subcortical plasticity following perceptual learning in a pitch
585         discrimination task. Journal of the Association for Research in Otolaryngology 12(1):89-
586         100.

587    Carey DP, Johnstone LT (2014) Quantifying cerebral asymmetries for language in dextrals and
588         adextrals with random-effects meta analysis. Frontiers in Psychology 5:1128.

589    Cha K, Zatorre RJ, Schönwiesner M (2016) Frequency selectivity of voxel-by-voxel functional
590         connectivity in human auditory cortex. Cerebral Cortex 26(1):211-224.

591    Chandrasekaran B, Kraus N (2010) The scalp-recorded brainstem response to speech: Neural
592         origins and plasticity. Psychophysiology 47(2):236-246.

593    Coffey EB, Herholz SC, Chepesiuk AM, Baillet S, Zatorre RJ (2016) Cortical contributions to
594         the     auditory     frequency-following     response     revealed     by     MEG. Nature
595         Communications 7(1):1-11.

596    Coffey EB, Musacchia G, Zatorre RJ (2017a) Cortical correlates of the auditory frequency-
597         following     and     onset     responses:     EEG     and     fMRI     evidence. Journal     of
598         Neuroscience 37(4):830-838.

599    Coffey EB, Chepesiuk AM, Herholz SC, Baillet S, Zatorre RJ (2017b) Neural correlates of
600         early sound encoding and their relationship to speech-in-noise perception. Frontiers in
601         Neuroscience 11:479.

602    Coffey EB, Nicol T, White-Schwoch T, Chandrasekaran B, Krizman J, Skoe E, Zotorre RJ,
603         Kraus N (2019) Evolving perspectives on the sources of the frequency-following
604         response. Nature Communications 10(1):1-10.

605    Cunningham J, Nicol T, Zecker SG, Bradlow A, Kraus N (2001) Neurobiologic responses to
606         speech in noise in children with learning problems: deficits and strategies for
607         improvement. Clinical Neurophysiology 112(5):758-767.

608    de Xivry JJ, Marko MK, Pekny SE, Pastor D, Izawa J, Celnik P, Shadmehr R (2011)
609         Stimulation of the human motor cortex alters generalization patterns of motor
610         learning. Journal of Neuroscience 31(19):7102-7110.

611 Dimitrijevic A, John MS, Picton TW (2004) Auditory steady-state responses and word
612    recognition scores in normal-hearing and hearing-impaired adults. Ear and
613    Hearing 25(1):68-84.

614 Encina-Llamas G, Harte JM, Dau T, Shinn-Cunningham B, Epp B (2019) Investigating the
615    effect of cochlear synaptopathy on envelope following responses using a model of the
616    auditory nerve. Journal of the Association for Research in Otolaryngology 20(4):363-
617    382.

618 Faria P, Hallett M, Miranda PC (2011) A finite element analysis of the effect of electrode area
619    and inter-electrode distance on the spatial distribution of the current density in
620    tDCS. Journal of Neural Engineering, 8(6):066017.

621 Ferrucci R, Marceglia S, Vergari M, Cogiamanian F, Mrakic-Sposta S, Mameli F, Zago S,
622    Babieri S, Priori A (2008) Cerebellar transcranial direct current stimulation impairs the
623    practice-dependent proficiency increase in working memory. Journal of Cognitive
624    Neuroscience 20(9), 1687-1697.

625 Filmer HL, Dux PE, Mattingley JB (2014) Applications of transcranial direct current
626    stimulation for understanding brain function. Trends in Neurosciences 37(12):742-753.

627 Fujihira H, Shiraishi K. (2015). Correlations between word intelligibility under reverberation
628    and speech auditory brainstem responses in elderly listeners. Clinical
629    Neurophysiology, 126(1), 96-102.

630 Gockel HE, Carlyon RP, Mehta A, Plack CJ (2011) The frequency following response (FFR)
631    may reflect pitch-bearing information but is not a direct representation of pitch. Journal
632    of the Association for Research in Otolaryngology 12(6):767-782.

633 Hartmann T, Weisz N (2019) Auditory cortical generators of the Frequency Following
634    Response are modulated by intermodal attention. NeuroImage 203:116185.

635 Herdman AT, Lins O, Van Roon P, Stapells DR, Scherg M, Picton TW (2002) Intracerebral
636    sources of human auditory steady-state responses. Brain Topography 15(2):69-86.

637 Holmberg EB, Hillman RE, Perkell JS (1988) Glottal airflow and transglottal air pressure
638    measurements for male and female speakers in soft, normal, and loud voice. The Journal
639    of the Acoustical Society of America 84(2):511-529.

640 Hornickel J, Kraus N (2013) Unstable representation of sound: a biological marker of
641    dyslexia. Journal of Neuroscience 33(8):3500-3504.

642 Hyde KL, Peretz I, Zatorre RJ (2008) Evidence for the role of the right auditory cortex in fine
643    pitch resolution. Neuropsychologia 46(2):632-639.

644  Jacobson L, Koslowsky M, Lavidor M (2012) tDCS polarity effects in motor and cognitive
645          domains: a meta-analytical review. Experimental Brain Research 216(1):1-10.

646  Krishnan A, Xu Y, Gandour JT, Cariani PA (2004) Human frequency-following response:
647          representation of pitch contours in Chinese tones. Hearing Research 189:1-12.

648  Krishnan A, Xu Y, Gandour J, & Cariani P (2005) Encoding of pitch in the human brainstem is
649          sensitive to language experience. Cognitive Brain Research 25(1):161-168.

650  Krishnan A, Gandour JT, Bidelman GM, Swaminathan J (2009) Experience dependent neural
651          representation of dynamic pitch in the brainstem. Neuroreport 20(4):408.

652  Kunze T, Hunold A, Haueisen J, Jirsa V, Spiegler A (2016) Transcranial direct current
653          stimulation changes resting state functional connectivity: a large-scale brain network
654          modeling study. NeuroImage 140:174-187.

655  Lehmann A., Schönwiesner M (2014) Selective attention modulates human auditory brainstem
656          responses: relative contributions of frequency and spatial cues. PloS One 9(1). e85442.

657  Luke R, De Vos A, Wouters J (2017) Source analysis of auditory steady-state responses in
658          acoustic and electric hearing. NeuroImage 147:568-576.

659  Mai G, Tuomainen J, Howell P (2018) Relationship between speech-evoked neural responses
660          and perception of speech in noise in older adults. The Journal of the Acoustical Society
661          of America 143(3):1333-1345.

662  Mai G, Schoof T, Howell P (2019) Modulation of phase-locked neural responses to speech
663          during different arousal states is age-dependent. NeuroImage 189:734-744.

664  Mathys C, Loui P, Zheng X, Schlaug G (2010) Non-invasive brain stimulation applied to
665          Heschl's gyrus modulates pitch discrimination. Frontiers in Psychology 1:193.

666  Matsushita R, Andoh J, Zatorre RJ (2015) Polarity-specific transcranial direct current
667          stimulation disrupts auditory pitch learning. Frontiers in Neuroscience 9:174.

668  Musacchia G, Sams M, Skoe E, Kraus N (2007) Musicians have enhanced subcortical auditory
669          and audiovisual processing of speech and music. Proceedings of the National Academy
670          of Sciences 104(40):15894-15898.

671  Nitsche M, Paulus W (2001) Sustained excitability elevations induced by transcranial DC
672          motor cortex stimulation in humans. Neurology 57(10):1899-1901.

673  Oldfield RC (1971) The assessment and analysis of handedness: the Edinburgh
674          inventory. Neuropsychologia 9(1):97-113.

675  Parbery-Clark A, Marmel F, Bair J, Kraus N (2011) What subcortical–cortical relationships tell
676          us about processing speech in noise. European Journal of Neuroscience 33(3):549-557.

677  Patterson RD, Uppenkamp S, Johnsrude IS, Griffiths TD (2002) The processing of temporal
678       pitch and melody information in auditory cortex. Neuron 36(4):767-776.

679  Penagos H, Melcher JR, Oxenham AJ (2004) A neural representation of pitch salience in
680       nonprimary human auditory cortex revealed with functional magnetic resonance
681       imaging. Journal of Neuroscience 24(30):6810-6815.

682  Presacco A, Simon JZ, Anderson S (2016) Evidence of degraded representation of speech in
683       noise, in the aging midbrain and cortex. Journal of Neurophysiology 116(5):2346-2355.

684  Puschmann S, Uppenkamp S, Kollmeier B, Thiel CM (2010) Dichotic pitch activates pitch
685       processing centre in Heschl's gyrus. NeuroImage 49(2):1641-1649.

686  Ranieri F, Podda MV, Riccardi E, Frisullo G, Dileone M, Profice P, Pilato F, Di Lazzaro V,
687       Grassi C (2012) Modulation of LTP at rat hippocampal CA3-CA1 synapses by direct
688       current stimulation. Journal of Neurophysiology, 107(7):1868-1880.

689  Reato D, Rahman A, Bikson M, Parra LC (2010) Low-intensity electrical stimulation affects
690       network dynamics by modulating population rate and spike timing. Journal of
691       Neuroscience 30(45):15067-15079.

692  Ross B, Picton TW, Pantev C (2002) Temporal integration in the human auditory cortex as
693       represented by the development of the steady-state magnetic field. Hearing
694       Research 165:68-84.

695  Ross B, Herdman AT, Pantev C (2005) Right hemispheric laterality of human 40 Hz auditory
696       steady-state responses. Cerebral Cortex 15(12):2029-2039.

697  Russo NM, Skoe E, Trommer B, Nicol T, Zecker S, Bradlow A, Kraus N (2008) Deficient
698       brainstem encoding of pitch in children with autism spectrum disorders. Clinical
699       Neurophysiology 119(8):1720-1731.

700  Salehinejad M, Kuo M, Nitsche M (2019) The impact of chronotypes and time of the day on
701       tDCS-induced  motor  cortex  plasticity  and  cortical  excitability. Brain
702       Stimulation 12(2):421.

703  Schochat E, Rocha-Muniz CN, Filippini R (2017) Understanding auditory processing disorder
704       through the FFR. In: The Frequency-Following Response: A Window into Human
705       Communication (Kraus N, Anderson S,, White-Schwoch T, Fay RR, Popper AN, eds),
706       pp225-250. Springer, Cham.

707  Sehm B, Schäfer A, Kipping J, Margulies D, Conde V, Taubert M, Villringer A, Ragert P
708       (2012) Dynamic modulation of intrinsic functional connectivity by transcranial direct
709       current stimulation. Journal of Neurophysiology 108(12):3253-3263.

Shah B, Nguyen TT, Madhavan S (2013) Polarity independent effects of cerebellar tDCS on short term ankle visuomotor learning. Brain Stimulation 6(6):966-968.

Skoe E, Kraus N (2010) Auditory brainstem response to complex sounds: a tutorial. Ear and Hearing 31(3):302.

Skoe E, Chandrasekaran B, Spitzer ER, Wong PC, Kraus N (2014) Human brainstem plasticity: the interaction of stimulus probability and auditory learning. Neurobiology of Learning and Memory 109:82-93.

Smalt CJ, Krishnan A, Bidelman GM, Ananthakrishnan S, Gandour JT (2012) Distortion products and their influence on representation of pitch-relevant information in the human brainstem for unresolved harmonic complex tones. Hearing Research 292:26-34.

Song JH, Skoe E, Banai K, Kraus N (2011) Perception of speech in noise: neural correlates. Journal of Cognitive Neuroscience 23(9):2268-2279.

Stagg CJ, Best JG, Stephenson MC, O'Shea J, Wylezinska M, Kincses ZT, Morris PG, Matthews PM, Johansen-Berg H (2009) Polarity-sensitive modulation of cortical neurotransmitters by transcranial stimulation. Journal of Neuroscience 29(16):5202-5206.

Strait DL, Kraus N, Skoe E, Ashley R (2009) Musical experience and neural efficiency: effects of training on subcortical processing of vocal expressions of emotion. European Journal of Neuroscience 29:661–668.

Unal G, Bikson M (2018) Transcranial Direct Current Stimulation (tDCS). In: Neuromodulation: Comprehensive Textbook of Principles, Technologies, and Therapies (Krames E, Peckham PH, Rezai AR, eds), pp1589-1610, Academic Press.

Vanvooren S, Hofmann M, Poelmans H, Ghesquière P, Wouters J (2015) Theta, beta and gamma rate modulations in the developing auditory system. Hearing Research 327:153-162.

White-Schwoch T, Carr KW, Thompson EC, Anderson S, Nicol T, Bradlow AR, Zecker SG, Kraus N (2015) Auditory processing in noise: A preschool biomarker for literacy. PLoS Biology 13(7):e1002196

Willems RM, Van der Haegen L, Fisher SE, Francks C (2014) On the other hand: including left-handers in cognitive neuroscience and neurogenetics. Nature Reviews Neuroscience 15(3):193-201.

Wong PC, Skoe E, Russo NM, Dees T, Kraus N (2007) Musical experience shapes human brainstem encoding of linguistic pitch patterns. Nature Neuroscience 10(4):420-422.

743    Zatorre RJ, Belin P (2001) Spectral and temporal processing in human auditory
744        cortex. Cerebral Cortex 11(10):946-953.